Journal Name

ARTICLE TYPE

Cite this: DOI: 10.1039/xxxxxxxxxx

The importance of current contributions to shielding constants in density-functional theory

Sarah Reimann,[a*] Ulf Ekström,[a‡] Stella Stopkowicz,[a] Andrew M. Teale,[a,b] Alex Borgoo,[a] and Trygve Helgaker [a¶].

Received Date
Accepted Date

DOI: 10.1039/xxxxxxxxxx

www.rsc.org/journalname

The sources of error in the calculation of nuclear-magnetic-resonance shielding constants determined by density-functional theory are examined. Highly accurate Kohn–Sham wave functions are obtained from coupled-cluster electron density functions and used to define accurate—but current independent—density-functional shielding constants. These new reference values, in tandem with high-accuracy coupled-cluster shielding constants, provide a benchmark for the assessment of errors in common density-functional approximations. In particular the role of errors arising in the diamagnetic and paramagnetic terms is investigated, with particular emphasis on the role of current-dependence in the latter. For carbon and nitrogen the current correction is found to be, in some cases, larger than 10 ppm. This indicates that the absence of this correction in general purpose exchange-correlation functionals is one of the main sources of errors in shielding calculations using density functional theory. It is shown that the current correction improves the shielding performance of many popular approximate DFT functionals.

1 Introduction

Nuclear-magnetic-resonance (NMR) shielding constants describe how an externally applied magnetic field is modified by the electrons surrounding the nuclei. The rich information contained in this response has made NMR spectroscopies a key tool in experimental chemistry. The prediction and interpretation of NMR spectra is therefore an important application area of quantum chemistry. Moreover, the sensitivity of this experimentally accessible shift represents a valuable test for the electronic-structure methodologies of quantum chemistry. In particular, for the applicability of Kohn–Sham density-functional theory (DFT), it is important to improve on the poor performance [1,2] of existing density-functional approximations (DFAs). From a DFT point of view, these calculations also represent an important theoretical challenge since the prediction of NMR shieldings relies on the induced electron current-density dependence of the exact exchange–correlation functional [3] or, alternatively, on its explicit dependence on the magnetic field. [4] The development of current-dependent DFAs remains an open problem. [5] In particular, it has been observed that the inclusion of a current dependence based on the free-electron-gas model does not lead to improved NMR shieldings. [6–9]

For the purpose of analyzing approximate schemes for the calculation of NMR shielding constants it is fruitful to write the shielding tensor as consisting of three terms,

$$\boldsymbol{\sigma} = \boldsymbol{\sigma}^{\mathrm{dia}} + \boldsymbol{\sigma}_{\rho}^{\mathrm{para}} + \boldsymbol{\sigma}_{\mathbf{j}}^{\mathrm{para}}. \tag{1}$$

The first term is the diamagnetic shielding (as defined in Section 2.1) which depends on the electron density ρ only. The second term is the current-independent part of the paramagnetic shielding (defined in Section 2.2), while the last term contains the current dependence. It has long been appreciated that, with the use of popular DFAs, the errors in $\boldsymbol{\sigma}^{\mathrm{dia}}$ are small, [10] and most development has been focused on improving the description of the paramagnetic shielding. [11–15] Until recently it has been assumed that $\boldsymbol{\sigma}_{\mathbf{j}}^{\mathrm{para}}$ can be neglected. [6] However, new theoretical and computational developments have allowed the importance of the current dependence of DFAs to be studied in isolation and it was found that these effects are not small compared with the total error of the best DFAs. [1] This observation constitutes an incentive to develop a current correction to the exchange–correlation functional of existing current-independent DFAs. Since the current corrections are expected to be relatively small it is important that errors in the underlying DFA are well balanced and minimized where possible. The aim of this paper is to quantify the magnitude of the current contribution, to analyze other sources of error (originating from the electron density in the diamagnetic shielding),

[a] Department of Chemistry, Centre for Theoretical and Computational Chemistry, University of Oslo, P.O. Box 1033, Blindern, Oslo N-0315, Norway
[b] School of Chemistry, University of Nottingham, University Park, Nottingham NG7 2RD, United Kingdom
∗ sarah.reimann@kjemi.uio.no
∗ ulf.ekstrom@kjemi.uio.no
∗ t.u.helgaker@kjemi.uio.no

and to suggest suitable DFAs to which further current corrections can be reliably applied.

We here study a collection of DFAs chosen to cover the familiar sequence consisting of the local-density approximation (LDA[16]), generalized-gradient approximation (GGA) functionals (BLYP[17,18] and PBE[19]), hybrid functionals (B97[20] and B3LYP[21]), and meta-GGA functionals (TPSS[22]). We also include the KT2 functional,[14] developed specifically for NMR shielding constants. Since a comparison with experiment requires a treatment of vibrational effects,[1] we compare instead with accurate theoretical shielding constants calculated at a fixed molecular geometry using coupled-cluster theory with single, double and perturbative triple excitations (CCSD(T)).[1]

The diamagnetic contribution to the shielding constant can be defined to depend only on the ground-state electron density. Therefore, we examine the error in the density calculated using different DFAs by comparison with the CCSD(T) reference density. In the absence of a field the exact exchange–correlation functional is purely density dependent. For such a purely density-dependent functional, which neglects current dependence but yields the exact charge density at zero field, the paramagnetic response is determined purely by the values of the orbitals and eigenvalues of the Kohn–Sham system. Using this fact we are able to calculate the $\boldsymbol{\sigma}_\rho^{\mathrm{para}}$ term in Eq. (1) and distinguish errors originating from the neglect of current dependence from those coming from the use of an approximate exchange–correlation functional.

2 Theory

2.1 NMR shielding constants

The NMR shielding tensor $\boldsymbol{\sigma}_K$ associated with nucleus K is defined as the second-order derivative of the molecular electronic energy with respect to the external magnetic field with flux density $\mathbf{B}$ and the magnetic moment $\mathbf{M}_K$ of that nucleus at $\mathbf{B}=0$ and $\mathbf{M}_K=0$,[23]

$$\boldsymbol{\sigma}_K = \left.\frac{\mathrm{d}^2 E}{\mathrm{d}\mathbf{B}\mathrm{d}\mathbf{M}_K}\right|_{\mathbf{B},\mathbf{M}_K=0}. \tag{2}$$

In common with all second-order magnetic properties, the shielding tensor can be decomposed into diamagnetic and paramagnetic parts,

$$\boldsymbol{\sigma}_K = \boldsymbol{\sigma}_K^{\mathrm{dia}} + \boldsymbol{\sigma}_K^{\mathrm{para}}, \tag{3}$$

but this decomposition is not unique. Throughout this work we use London atomic orbitals to ensure gauge origin independence of our results. We follow the convention that the diamagnetic part depends only on the ground-state density; all terms describing some form of response to the field, including the response encoded in the London atomic orbitals or gauge-invariant atomic orbitals (GIAOs), are contained in the paramagnetic part.[24] Specifically, we define the diamagnetic part as (omitting here and elsewhere the summation over electrons)

$$\boldsymbol{\sigma}_K^{\mathrm{dia}} = \frac{1}{2}\left\langle 0 \left| \frac{\mathbf{r}_{\mathrm{O}}^{\mathrm{T}}\mathbf{r}_K - \mathbf{r}_{\mathrm{O}}\mathbf{r}_K^{\mathrm{T}}}{r_K^3} \right| 0 \right\rangle, \tag{4}$$

where $\mathbf{r}_K = \mathbf{r} - \mathbf{R}_K$ is the position vector of the electron relative that of the nucleus $\mathbf{R}_K$, and $\mathbf{r}_{\mathrm{O}} = \mathbf{r} - \mathbf{R}_{\mathrm{O}}$ is the position vector of the electron relative to the gauge origin $\mathbf{R}_{\mathrm{O}}$. Unless otherwise stated, atomic units are used in this paper. Setting the gauge origin at nucleus K, the diamagnetic NMR shielding constant becomes directly proportional to the expectation value of the Coulomb interaction at the nucleus

$$\sigma_K^{\mathrm{dia}} = \frac{1}{3}\mathrm{Tr}\boldsymbol{\sigma}_K^{\mathrm{dia}} = \frac{1}{3}\left\langle 0 \left| \frac{1}{r_K} \right| 0 \right\rangle. \tag{5}$$

In the present paper, the quality of the total shielding constant σ_K and its diamagnetic part σ_K^{dia} calculated with different DFAs will be assessed by a direct comparison with accurate CCSD(T) values, thereby quantifying also the error in the paramagnetic part σ_K^{para}. We also analyze the sources of error in σ_K^{para} and, in particular, quantify the error incurred by neglecting the field dependence of the exchange–correlation functional, as discussed in the following subsection.

2.2 Magnetic perturbations in current-independent DFT

Here we are concerned only with pure density functionals, i.e. LDA, GGA, and the exact universal functional. When the current dependence of the exchange–correlation energy is neglected, the ground-state energy can be decomposed into familiar components: the non-interacting kinetic energy $T_{\mathrm{s}}(\rho,\mathbf{A})$ with a dependence on the vector potential $\mathbf{A}$, the exchange–correlation–Hartree energy $E_{\mathrm{xcH}}(\rho)$, and the interaction between the electrons and the external scalar potential v set up by the nuclei, (v,ρ):

$$E(v,\mathbf{A}) = \inf_\rho \{T_{\mathrm{s}}(\rho,\mathbf{A}) + E_{\mathrm{xcH}}(\rho) + (\rho,v) \,|\, \textstyle\int \rho(\mathbf{r})\,\mathrm{d}\mathbf{r} = N\}. \tag{6}$$

Note that within this approximation, E_{xcH} here remains the standard "non-magnetic" exchange–correlation–Hartree energy.

We now show that, for a current independent functional of the above form, the second derivative with respect to the vector potential is simply the second derivative of the non-interacting kinetic energy. Assuming the existence of a minimizing density $\rho_{\mathrm{GS}}(v,\mathbf{A})$ and that the derivatives are well defined (for a discussion of this point in conventional DFT see Ref.[25]), the DFT Euler equation is given by

$$\frac{\delta}{\delta\rho(\mathbf{r})}\left(T_{\mathrm{s}}(\rho,\mathbf{A}) + E_{\mathrm{xcH}}(\rho)\right) + v(\mathbf{r}) = \mu. \tag{7}$$

For closed-shell systems (which are considered here), the first derivative of T_{s} with respect to $\mathbf{A}$ vanishes since $T_{\mathrm{s}}(\rho,\mathbf{A})$ is an even function of $\mathbf{A}$ at $\mathbf{A}=\mathbf{0}$. The Euler equation is therefore automatically satisfied to first order in $\mathbf{A}$, implying that the density depends on $\mathbf{A}$ only to second order. Setting $\rho = \rho_0 + \rho_2\mathbf{A}^2$ and ex-

panding the ground-state energy to second order in $\mathbf{A}$, we obtain

$$E(v,\mathbf{A}) = T_s(\rho_0,0) + E_{\mathrm{xcH}}(\rho_0) + (\rho_0, v) + \frac{1}{2}\iint \left.\frac{\delta^2 T_s(\rho,\mathbf{A})}{\delta\mathbf{A}(\mathbf{r})\delta\mathbf{A}(\mathbf{r}')}\right|_{(\rho_0,0)} \mathbf{A}(\mathbf{r})\mathbf{A}(\mathbf{r}')\mathrm{d}\mathbf{r}\mathrm{d}\mathbf{r}' + \int \left(\left.\frac{\delta\left(T_s(\rho,\mathbf{A}) + E_{\mathrm{xcH}}(\rho)\right)}{\delta\rho(\mathbf{r})}\right|_{(\rho_0,0)} + v(\mathbf{r})\right) \rho_2(\mathbf{r})\mathbf{A}(\mathbf{r})^2 \mathrm{d}\mathbf{r}, \quad (8)$$

where the last term vanishes because the Euler equation is satisfied for the reference state; since the density variations are particle-number preserving for all $\mathbf{A}$, the integral $\mu\int\rho_2(\mathbf{r})\mathbf{A}^2(\mathbf{r})\,\mathrm{d}\mathbf{r}$ vanishes. Hence, the second derivative of a closed-shell ground-state energy with respect to the vector potential, at zero vector potential, is simply the second derivative of the non-interacting kinetic energy. Note that the exchange–correlation kernel contributions, arising from the second derivative of E_{Hxc}, appear only at higher orders in $\mathbf{A}$. This well-known result is usually stated for LDA and GGA functionals in terms of the "magnetic Hessian".[26] The present proof relies only on the observation that T_s is even in $\mathbf{A}$ at $\mathbf{A}=\mathbf{0}$.

For the shielding tensor, we then insert $\mathbf{A} = \mathbf{A}_0 + \mathbf{A}_K$, where $\mathbf{A}_0$ and $\mathbf{A}_K$ are the vector potentials associated with $\mathbf{B}$ and $\mathbf{M}_K$, respectively, to obtain the usual formula in terms of Kohn–Sham orbitals and eigenvalues. Neglecting the contribution due to London orbitals the expression is[6]

$$\boldsymbol{\sigma}_p^{\mathrm{para}} = -\sum_i^{\mathrm{occ}}\sum_a^{\mathrm{virt}} \frac{\langle i|\mathbf{l}|a\rangle\langle a|\mathbf{l}_K^T r_K^{-3}|i\rangle + \mathrm{h.c.}}{\varepsilon_a - \varepsilon_i}, \quad (9)$$

where h.c. is the hermitian conjugate and $\mathbf{l}$ is the angular momentum operator.

It should be noted that by employing Eq. (8) the shielding tensor (or indeed other magnetic properties) can be computed for an arbitrary input density without knowledge of the exact exchange-correlation (XC) functional. All that is required are the second derivatives of T_s, which can be obtained from the Kohn–Sham wave function corresponding to ρ. This wave function can be obtained by various approaches, for example the Zhao–Morrison–Parr[27] method employed by Wilson and Tozer[13] for the calculation of shieldings. We instead use the method outlined in Section 3.

3 Computational Details

We have evaluated total and diamagnetic NMR shielding constants for a set of small atoms and molecules, at the CCSD(T) equilibrium geometries. In the next section, we compare wave-function quantities from Hartree–Fock (HF) theory, second-order Møller–Plesset (MP2) perturbation theory, and CCSD(T) theory with those from a representative set of standard DFAs. To quantify the error arising from the neglect of the current dependence in the DFA, we also present Kohn–Sham shielding constants obtained from accurate CCSD(T) densities using an established inversion scheme.[28,29]

The coupled-cluster calculations of shielding constants were performed using CFOUR.[30] A development version of DALTON[31,32] was used for all other calculations, except those involving the TPSS functional. The latter were evaluated with the LONDON quantum-chemistry software.[8,33,34]

Meta-GGAs, such as TPSS, depend on the Kohn–Sham kinetic energy density $\tau_0(\mathbf{r}) = \frac{1}{2}\sum_i^{\mathrm{occ}} \|\nabla\phi_i(\mathbf{r})\|^2$. In magnetic fields this quantity must be generalized in a gauge-invariant fashion. Maximoff and Scuseria[35] suggested the use of the physical kinetic energy density

$$\tau_{\mathrm{MS}} = \tau_0 + \mathbf{j}_p\cdot\mathbf{A} + \frac{1}{2}\rho\mathbf{A}^2. \quad (10)$$

This quantity is gauge invariant but introduces an explicit dependence of the XC energy on the vector potential $\mathbf{A}$. Another problem is that the so-called "isoorbital indicator" used in the TPSS functional can take unphysical values in magnetic fields.[36] We denote the TPSS functional with this choice of τ by cTPSS(τ_{MS}). Another option is to use the gauge-invariant kinetic energy proposed by Dobson,[37] and used by Becke[38] and Tao,[39]

$$\tau_{\mathrm{D}} = \tau_0 - \frac{\mathbf{j}_p^2}{2\rho}. \quad (11)$$

This kinetic energy density depends only on the paramagnetic current, and not on the external magnetic field. It also leads to physical isoorbital indicator values. This functional, here denoted cTPSS(τ_{D}), is equivalent to that introduced by Bates and Furche for the calculation of excitation energies in Ref.[40] and its implementation and application to magnetic properties will be discussed in detail elsewhere.[41] For reference we also compute shielding values using the gauge dependent τ_0, with the gauge origin placed on the molecular center of mass. We refer to this functional as TPSS(τ_0). The shielding constants with the TPSS and cTPSS functionals presented in this work were obtained by a numerical differentiation, using finite magnetic fields – for further details see Ref.[8].

We used the augmented correlation-consistent basis sets by Dunning and coworkers, known to be suitable for the computation of magnetic properties.[42] We investigated basis-set convergence and found the aug-cc-pVQZ basis[43,44] to be appropriate for the systems studied in this work. Cartesian Gaussian basis sets have been used throughout all calculations.

To ensure gauge-origin independence of the total shieldings, we employ London orbitals.[45,46] We note that the DALTON program uses a definition for the diamagnetic part of the NMR shielding constant that includes a contribution from the London atomic orbitals. We here use the definition in Eq. (4), where we obtain the corresponding values using separate calculations without London orbitals.

In order to isolate the effect of the current dependent exchange-correlation energy on the shieldings we calculate the non-interacting Kohn–Sham potential, orbitals and orbital energies corresponding to a specific electron density using the procedure of Wu and Yang.[28] The paramagnetic shielding constants are then obtained using Eq. (9). These calculations were carried out using a locally modified version of the DALTON program.[29] Total shield-

ing constants calculated using this method will be called σ_{KS} in the following.

4 Results and discussion

In this section, we analyze the errors coming from the diamagnetic and the paramagnetic parts of the NMR shieldings to gain insight into the limitations of common DFAs and the role of current dependence. We study a set of small systems (He, Ne, HF, CO, N_2, H_2O, NH_3, and CH_4) for which we computed accurate CCSD(T) reference values, and also obtained the corresponding accurate Kohn–Sham non-interacting wave functions.

4.1 Current-dependence of DFT shielding constants

We begin by assessing the importance of $\sigma_{\mathbf{j}}^{\text{para}}$ relative to the diamagnetic and current-independent contributions to the shielding constant in Eq. (1) for the molecules in the test set, see Table 1. In this table, σ is the total shielding constant calculated using CCSD(T) theory and the diamagnetic part σ^{dia} is the expectation value in Eq. (4) calculated from the CCSD(T) density matrix. To obtain the paramagnetic density and current contributions, we have first calculated the total current free shielding constant σ_{KS} using the Wu–Yang scheme with the CCSD(T) density as described in Section 3 and then used the relations $\sigma_{\rho}^{\text{para}} = \sigma_{KS} - \sigma^{\text{dia}}$ and $\sigma_{\mathbf{j}}^{\text{para}} = \sigma - \sigma_{KS}$.

From Table 1, we first note that the current contribution is typically one to two orders of magnitude smaller than the dia- and paramagnetic contributions to the shielding constants. However, since the dia- and paramagnetic contributions are always of opposite sign and may nearly cancel, the current contribution to the shielding cannot always be neglected and sometimes becomes important. For example, in σ_C in CO, the total shielding is 5.4 ppm with a current contribution of 11.0 ppm, twice as large as the total shielding; in this particular case, the total dia- and paramagnetic contributions are 327.0 and −332.6 ppm. In N_2, the situation is similar but less dramatic, the total shielding constant being −57.4 ppm with a large current contribution of 13.3 ppm. Clearly, the current contribution to the shielding constants cannot in general be neglected, at least for heavy atoms: for the non-hydrogen atoms in Table 1, the current contribution ranges from 1.7 to 13.3 ppm. For proton shieldings, the current contribution is negligible, contributing in all cases less than 1% to the total shielding constant. Although our estimated error, due to approximation in the Wu–Yang procedure, on the current contribution lies below 0.05 ppm for the H atom, we cannot be completely confident that the negative sign of the current contribution for this atom is not a basis set error. For the other atoms the current contribution is clearly positive.

The main source of error in the calculated $\sigma_{\mathbf{j}}^{\text{para}}$ values arise from the orbital and potential basis sets, as well as optimization thresholds, employed in the Wu–Yang calculations. By studying the convergence of the results in terms of the potential and orbital basis sets (we use the same family of aug-cc-pVXZ sets for both) when going between the QZ and 5Z sets we can estimate the errors in Table 1, which are listed in the last column of the same table. The by far largest error, most likely smaller than 1.5 ppm, is in the current contribution for N_2, but this and other errors do not change any conclusion or has any significant impact on the statistic in the following sections.

Finally, we note that the current contribution is positive for all heavy atoms in Table 1, increasing the shielding constant and reducing the overall paramagnetic contribution. For the protons, by contrast, the current contribution is negative in all cases. We cannot rule out that the very small negative current contribution for proton is a numerical artifact; however, this seems unlikely in view of the high degree of convergence for the proton shielding of the HF molecule. It appears, therefore, that the current contribution to shielding constants can be both negative and positive.

4.2 Diamagnetic shielding constants and the role of the electron density

Since the current contribution to the shieldings in the previous subsection was shown to sometimes be as large as 10 ppm it would be a worthwhile effort to develop an approximate DFT expression for this correction. For this reason it is important to investigate the sources of errors in the diamagnetic and paramagnetic contributions for existing DFAs. For an evaluation of the diamagnetic shielding constants, we compare calculated DFA, HF, and MP2 diamagnetic contributions to the shielding constants with the corresponding CCSD(T) values. In Table 2, we report the mean and standard deviation of the error in σ^{dia} for the different models. Although only a limited number of systems are considered the methods can be qualitatively ranked, in order from smallest to largest absolute errors, as CCSD, MP2 < PBE, B3LYP, B97, BLYP, TPSS, HF < LDA < KT2. Note that both forms of cTPSS give the same result as TPSS, since the diamagnetic shielding is defined as not including any current effects. The most remarkable observation is that the KT2 functional, which has been optimized for improving *total* NMR shielding constants, gives an error in the *diamagnetic* shielding at least an order of magnitude larger than all other methods. We note that the hybrid functionals B3LYP and B97 and the meta-GGA functional TPSS are not significantly better than the best GGA functionals, but most DFAs are clearly outperformed by MP2 theory. The exception is PBE, which gives very high quality diamagnetic shieldings for our test set.

Although the diamagnetic part of the shielding constant is the focus of this section, it is just one measure of a "good density". Exchange–correlation functionals are typically optimized for ground-state energies, which include the expectation value $\langle r^{-1} \rangle$. We therefore expect these functionals to give good diamagnetic shieldings, but it is nevertheless worthwhile to investigate the density error in more detail. In the paramagnetic part of the shielding [Eq. (9)] the presence of the r^{-3} operator is expected to give larger weights to density errors near the nucleus, compared to the diamagnetic term.

We therefore investigate the electron density errors of the different methods in a more general sense. In Figure 2 the density errors $\Delta\rho(r)$, $r\Delta\rho(r)$, $r^2\Delta\rho(r)$ and $r^4\Delta\rho(r)$ are plotted as functions of r (where $\Delta\rho = \rho - \rho_{\text{CCSD(T)}}$) for the helium and neon atoms. The first of these shows the local density error at different locations in the atom, and integrates to the expectation value $\langle r^{-2} \rangle$.

Table 1 The diamagnetic, current independent paramagnetic and current dependent paramagnetic parts of the benchmark shielding constants in ppm, calculated at the CCSD(T) level, together with estimates of the absolute error due to the Wu-Yang procedure.

Molecule	σ	=	σ^{dia}	+	$\sigma_{\rho}^{\mathrm{para}}$	+	$\sigma_{\mathbf{j}}^{\mathrm{para}}$	Err
He	59.9		59.9		0		0	0
Ne	552.0		552.0		0		0	0
HF(H)	28.9		108.6		−79.5		−0.2	0.05
CH_4(H)	31.3		87.7		−56.3		−0.1	0.05
NH_3(H)	31.5		95.5		−63.9		−0.1	0.05
H_2O(H)	30.8		102.4		−71.4		−0.2	0.05
CH_4(C)	199.4		297.0		−104.9		7.3	0.05
CO(C)	5.4		327.0		−332.6		11.0	0.05
NH_3(N)	270.7		354.5		−89.4		5.6	0.5
N_2(N)	−57.4		384.7		−455.4		13.3	1.5
H_2O(O)	337.8		416.2		−82.0		3.6	0.2
CO(O)	−51.7		444.8		−501.0		4.5	0.5
HF(F)	420.8		482.1		−63.0		1.7	0.5

Table 2 Mean absolute density error I (Eq. 12), mean and standard deviation (S) of the shielding error (in ppm) $\Delta\sigma^{\mathrm{dia}} = \sigma^{\mathrm{dia}} - \sigma^{\mathrm{dia}}_{\mathrm{CCSD(T)}}$ (left), $\Delta\sigma = \sigma - \sigma_{\mathrm{CCSD(T)}}$ (middle) and $\Delta\sigma_{\mathrm{KS}} = \sigma - \sigma_{\mathrm{KS}}$ (right). Here σ_{KS} is the current independent DFT shielding computed from the CCSD(T) densities. This method is also labeled KS(CCSD(T)) in the table. The I value for TPSS and cTPSS was omitted for technical reasons.

Method	I	$\Delta\sigma^{\mathrm{dia}}$	S($\Delta\sigma^{\mathrm{dia}}$)	$\Delta\sigma$	S($\Delta\sigma$)	$\Delta\sigma_{\mathrm{KS}}$	S($\Delta\sigma_{\mathrm{KS}}$)
LDA	0.14	−1.01	0.53	−9.60	14.61	−6.02	11.50
BLYP	0.13	0.19	0.15	−9.62	11.36	−6.04	7.71
PBE	0.08	0.03	0.11	−8.58	10.91	−5.00	7.61
KT2	0.13	2.51	1.66	−2.00	4.14	1.58	5.16
B97	0.05	0.15	0.05	−9.18	11.79	−5.60	8.39
B3LYP	0.07	0.11	0.09	−10.36	13.32	−6.78	9.65
TPSS(τ_0)	-	0.22	0.09	−4.44	4.68	−0.86	2.95
cTPSS(τ_{D})	-	0.22	0.09	-7.15	8.29	-3.57	4.92
cTPSS(τ_{MS})	-	0.22	0.09	-6.57	7.20	-2.99	3.87
HF	0.14	−0.15	0.34	−11.59	17.85		
MP2	0.03	−0.01	0.09	3.80	5.10		
CCSD	0.02	0.01	0.04	−1.28	2.03		
KS(CCSD(T))	0	0	0	−3.57	4.59		

The second quantity integrates to the error in the expectation value $\langle r^{-1} \rangle$, while the third integrates to the error in the number of electrons (which is zero), and the fourth integrates to the error in the atomic quadrupole moment.

Considering the maximum error at different r in the two first rows of Figure 2, rather than the average error appearing in the diamagnetic shielding integral, we obtain a ranking CCSD < MP2 < TPSS, HF < PBE, B3LYP, B97, BLYP < KT2 < LDA. The CCSD error is not plotted, to reduce visual clutter, but this error is in all cases smaller than that of all other methods. For simplicity the GGA functionals are not distinguishable in the figure, but the overall trends and spread are clearly visible. In particular, the density error near the nucleus is very large for all DFAs. However, this error is cancelled by opposite errors further away from the nucleus, leading overall to good accuracy of the $\langle r^{-1} \rangle$ expectation value relevant for the diamagnetic shielding.

From the different weightings shown in Figure 2, we conclude that a similar trend holds for the quadrupole moments. However, the advantage of HF is now less pronounced and the KT2 error less severe. The TPSS functional loses its advantage over the other DFAs in the regions far away from the nucleus, but these are less relevant for shieldings. We note that a radial density analysis has recently been utilized to understand density errors associated with the correlation treatment in DFAs in Refs.[47,48]. Our density study differs slightly in the choices of functionals, and importantly includes data for the TPSS meta-GGA functional. This functional is found to be the best performing DFA in our benchmark. While it has the same error trends (i.e. too large density at the nucleus and similar density error oscillations away from the nucleus) as the GGA functionals it has the smallest absolute errors and more mild oscillations. Since the HF density errors often are of opposite sign to the DFA errors one might think that hybrid functionals would be good overall performers. This is not the case for the B3LYP functional, which gives results in line with the pure GGA functionals.

Figure 1 shows the error $\Delta\rho$ along the bond axis for the N_2 and H_2O molecules. In both cases, it is clear that there exist regions near the nuclei, up to the inner-valence region, where the Kohn-Sham calculations yield densities considerably worse than HF. However, as can be seen from the mean of the integral of the absolute density errors,

$$I = \int |\rho(\mathbf{r}) - \rho_{\mathrm{CCSD(T)}}(\mathbf{r})| \mathrm{d}\mathbf{r}, \qquad (12)$$

presented in Table 2, the global density error is somewhat smaller for the approximate Kohn-Sham calculations. BLYP has a similar absolute error I as HF, but since the errors at a particular point in space often have opposite sign (see Fig. 2) it is not surprising that the hybrid functional B3LYP reduces the value of I significantly. However, the pure GGA functionals PBE and B97 both perform similar to, or better than, B3LYP by the same measure. However, the value of I seems to be only weakly correlated with the quality of the diamagnetic shielding. The KT2 functional has a large diamagnetic error but the value of I is not larger than for BLYP. This emphasizes the physical fact that it is the density near each atomic nucleus which is important for the shielding of that particular nucleus.

The reason that the DFAs perform better than the HF method according to these measures is that the errors, while large, are localized to small regions near the nuclei. Furthermore, the density errors oscillate about zero as we move away from the nucleus, as seen in Figure 1. Around the nuclei all DFA densities show a much larger error than the HF method; however, as we move away from the nuclei, the DFA densities improve relative to the HF density. It should also be pointed out that the absolute value of the DFA error is about two orders of magnitude larger in the core region than in the valence region. In other words, the HF density has, relative to the CCSD(T) density, a more uniform error, whereas the DFAs perform better in the valence region but are much worse in the core region.

To summarize this section we note that for the worst performing functionals for the diamagnetic shieldings (LDA and KT2) the plot of the density errors clearly show the origin of their poor diamagnetic performance. However, investigating the PBE densities, which give the best diamagnetic shieldings of all the tested DFAs, reveals that this good performance is a result of error cancellation. The TPSS functional, on the other hand, has smaller maximum errors and its gauge-independent cTPSS variants may be a more promising functional for shieldings, considering the (here unquantified) effect of the core density on the paramagnetic shielding tensor.

Finally we note that, for the considered molecules, MP2 gives densities that are of much higher quality than all considered DFAs, but as can be seen in Table 2 such high quality densities are not needed for high (i.e. sub-ppm) accuracy in the diamagnetic shielding constants.

4.3 Total NMR shielding constants

Table 2 contains the mean and standard deviation of the error in the NMR shielding constant for the different methods. We first consider the error with respect to the CCSD(T) shieldings ($\Delta\sigma$ in columns five and six), which include current contributions. One should note that the CO and N_2 molecules are the most difficult cases for all the methods. This means that the average error is strongly influenced by these two molecules, emphasizing the molecules with the largest errors.

Regarding the error in the total shielding, we obtain a ranking CCSD < KT2, MP2 < TPSS(τ_0), cTPSS(τ_{MS}), cTPSS(τ_{D}) < PBE, B97, BLYP < B3LYP, LDA < HF. The KT2 exchange–correlation functional clearly benefits from having been constructed by fitting to experimental shielding data, performing well for total shielding constants in spite of its poor performance for the diamagnetic part. The KT2 errors have roughly equal contributions from the diamagnetic and paramagnetic parts, whereas the error in the paramagnetic term dominates for all other DFAs, among which TPSS(τ_0) is a clear winner.

Surprisingly, the current including, gauge-independent variants of cTPSS both perform slightly worse than TPSS(τ_0), although they still give better values than the remaining DFAs. Since τ_0 depends on the choice of gauge the TPSS(τ_0) functional cannot be recommended for general use, but the results seem relatively in-

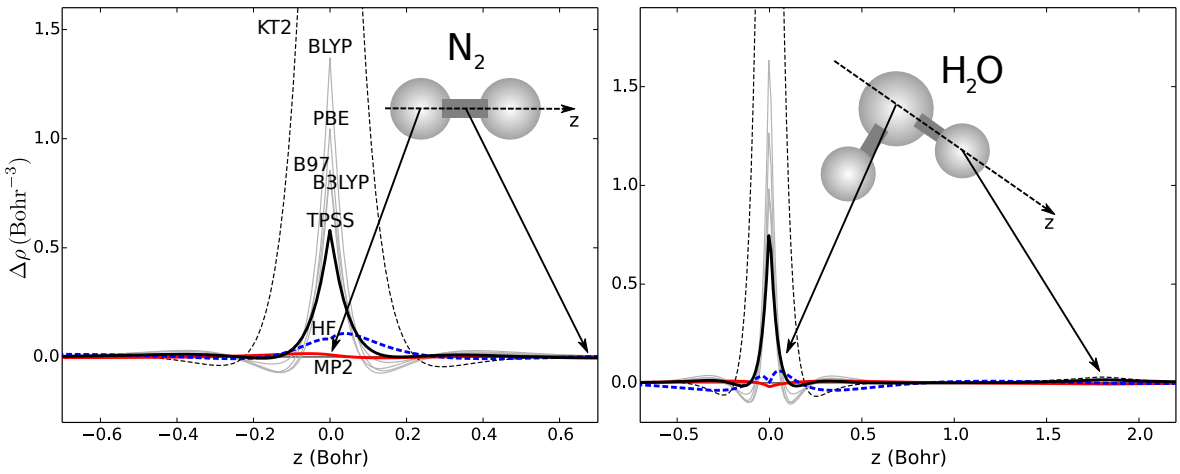

Fig. 1 The density error $\Delta\rho = \rho - \rho_{\mathrm{CCSD(T)}}$ for N_2 and H_2O is plotted along the molecular axis and O-H bond respectively. Line types are the same as in Fig. 2

sensitive to small shifts in gauge origin. Moving the gauge origin from the center of mass to the shielding nucleus in N_2 resulted in a shielding shift of 0.7 ppm for TPPS(τ_0).

The last row of the table shows the performance of the KS(CCSD(T)) functional. This is in fact the current-independent shielding σ_{KS} computed using the CCSD(T) density. This functional is a close approximation to the shielding that would be obtained from an exact, but current independent, DFT shielding calculation. One sees that the error is surprisingly slightly larger than the error of the KT2 functional. The reason that KT2 stands out from all other DFAs is that it has been directly fitted to experimental shielding data. It is evident from the diamagnetic performance and density error of KT2 that this fitting procedure has lead to improved total shielding constants, but has introduced other sources of errors in the functional. An improved functional, KT3,[15] which remedies some of these errors, was later introduced. However, KT3 does not give improved shielding constants, and the authors remark that it gives rather poor electronic energies. Since these energies contain the same expectation value $\langle r^{-1} \rangle$ as the diamagnetic shielding constants it is likely that KT3 suffers from the same diamagnetic errors as KT2.

4.4 Importance of current contributions to the exchange-correlation energy

The method rankings in the last subsection, including the ranking of the MP2 method, are very similar to those obtained for carbon and hydrogen by Flaig *et al.*[2] The DFA benchmark we have just discussed is however flawed for our purpose, because current independent DFAs are compared to reference numbers which include current effects. If a current correction is developed it should be applied to a base functional that gets as close as possible to the *current independent* shielding $\sigma_{\mathrm{KS}} = \sigma^{\mathrm{dia}} + \sigma_{\rho}^{\mathrm{para}}$. Therefore we have re-evaluated the performance of the DFAs benchmarked in the previous section against the σ_{KS} numbers computed using CCSD(T) electron densities. The results are found in the two rightmost columns of Table 2. The most striking feature of these columns is that the performance of all DFAs, but one, improve significantly. The standard deviations decrease by about 2 ppm, and the average error decreases in magnitude by about 3-4 ppm. The exception is KT2, which has a nearly unchanged average error but an increase in the standard deviation by about 1 ppm.

Using the current independent reference values the ranking of the DFAs changes. The best functional is now TPSS(τ_0), followed by cTPSS, while the best GGA functional is PBE. It is noteworthy that, again, the gauge-dependent TPSS(τ_0) performs better than cTPSS. The reasons for that need to be explored in future work. KT2 is now the second best functional overall, but in contrast to the other functionals the current correction actually worsens its performance.

The cTPSS functional is clearly an interesting case since it already includes a current correction and so direct comparison with the current independent benchmark values is not appropriate. The current correction in cTPSS(τ_{D}), arises naturally in the Taylor expansion of the spherically averaged exchange hole as shown by Dobson.[37] Unfortunately, since the current dependence in cTPSS cannot be easily disentangled from the requirement for gauge-invariance of E_{xc}, it is not easy to quantify the extent to which the treatment of current effects is complete, nor how these corrections interact with errors already present in the underlying exchange-correlation functional form. Further investigation of these points, including the worse performance of cTPSS compared to TPSS, is left to further work. Nonetheless, it is noteworthy that cTPSS performs better than all DFAs except KT2 when compared with CCSD(T) data. The quality of the current corrected results can be compared to MP2, although it tends to underestimate shielding constants by a similar extent to which MP2 overestimates.

5 Conclusions

By directly calculating the exchange correlation current contribution to NMR shielding constants (using CCSD(T), together with the Wu–Yang method of obtaining the corresponding Kohn–Sham system) we have shown that the current contribution can in some cases amount to more than 10 ppm for carbon and nitrogen

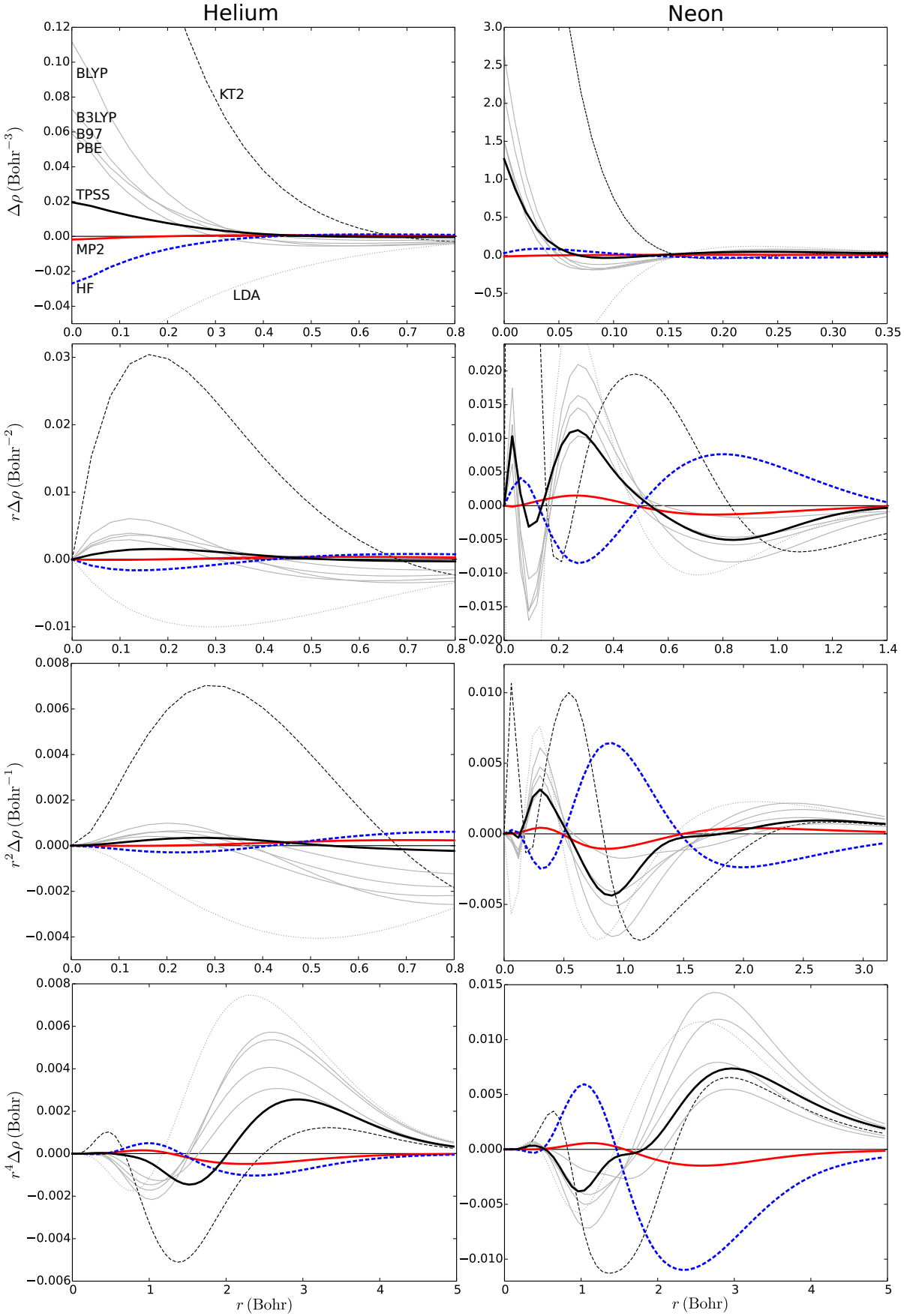

Fig. 2 The density error $\Delta\rho = \rho - \rho_{\mathrm{CCSD(T)}}$ with weightings (from top to bottom) 1, r, r^2 and r^4, for the helium (left) and neon (right) atoms. The integral of the plotted functions corresponds to errors in the expectation value of $\langle 1/r^2\rangle$, $\langle 1/r\rangle$, $\langle 1\rangle$ (particle number) and $\langle r^2\rangle$, respectively. LDA is drawn using a thin dotted gray line, BLYP, B3LYP, PBE and B97 using solid thin gray line, KT2 thin dashed black line, TPSS black, HF dashed blue, MP2 red. The gray lines (GGA and hybrid functionals) are not intended to be distinguishable in this figure. Note the different scales in each subplot.

atoms. This means that the missing current contribution may be one of the leading causes of errors in shielding calculations using approximate DFT functionals. This also suggests that current independent functionals should be judged based on their ability to reproduce accurate *ab initio* numbers with the current contribution subtracted. As shown in Section 4.4 this reduces the average errors in the functionals by several ppm. The exception is the empirical KT2 functional, which was fitted to experimental shielding data. As such the functional already implicitly includes an empirical current correction, and it fits better to the current including benchmark set than the current free one.

In order to understand the large errors made by KT2 in the diamagnetic part of the shielding constant we have studied the ground state electron density for helium, neon, CO and N_2. The origin of the errors in KT2 diamagnetic shieldings is clearly seen in the density, which has a very large error within 0.2 Bohr of the nucleus. The standard GGA functionals, and PBE in particular, give excellent diamagnetic shieldings, but still have large density error oscillations near the nucleus. Here TPSS stands out as the exchange-correlation functional with the most balanced density error. The MP2 methods gives densities with much smaller maximum error than any density functional approximation, but for our test set of molecules this high accuracy is not needed for the purpose of NMR shieldings.

For our (fairly small) benchmark set the current corrected cTPSS functional provides results of similar quality to MP2. These results suggest that current dependent meta-GGA functionals such as cTPSS may provide a good base for the further development of DFAs for use in CDFT. The extent to which remaining errors in these functionals can be attributed to the incomplete treatment of current effects or errors in the underlying exchange–correlation functional form will be investigated in future work. To make further progress it may be necessary to address both aspects simultaneously.

Acknowledgments

This work was supported by the Norwegian Research Council through the CoE Centre for Theoretical and Computational Chemistry (CTCC) Grant Nos. 179568/V30 and 171185/V30 and through the European Research Council under the European Union Seventh Framework Program through the Advanced Grant ABACUS, ERC Grant Agreement No. 267683. A.M.T. is also grateful for support from the Royal Society University Research Fellowship scheme.

References

1 A. M. Teale, O. B. Lutnæs, T. Helgaker, D. J. Tozer and J. Gauss, *J. Chem. Phys.*, 2013, **138**, year.

2 D. Flaig, M. Maurer, M. Hanni, K. Braunger, L. Kick, M. Thubauville and O. C., *J. Chem. Theory Comput.*, 2014, **10**, 572–578.

3 G. Vignale and M. Rasolt, *Phys. Rev. Lett.*, 1987, **59**, 2360–2363.

4 C. J. Grayce and R. A. Harris, *Phys. Rev. A*, 1994, **50**, 3089–3095.

5 E. I. Tellgren, S. Kvaal, E. Sagvolden, U. Ekström, A. M. Teale and T. Helgaker, *Phys. Rev. A*, 2012, **86**, 062506.

6 A. M. Lee, N. C. Handy and S. M. Colwell, *J. Chem. Phys.*, 1995, **103**, 10095–10109.

7 W. Zhu and S. B. Trickey, *J. Chem. Phys.*, 2006, **125**, 094317.

8 E. I. Tellgren, A. M. Teale, J. W. Furness, K. K. Lange, U. Ekström and T. Helgaker, *J. Chem. Phys.*, 2014, **140**, 034101.

9 W. Zhu, L. Zhang and S. B. Trickey, *Phys. Rev. A*, 2014, **90**, 022504.

10 G. Schreckenbach and T. Ziegler, *J. Phys. Chem.*, 1995, **99**, 606–611.

11 V. G. Malkin, O. L. Malkina, M. E. Casida and D. R. Salahub, *J. Am. Chem. Soc.*, 1994, **116**, 5898–5908.

12 P. J. Wilson, R. D. Amos and N. C. Handy, *Mol. Phys.*, 1999, **97**, 757–768.

13 P. J. Wilson and D. J. Tozer, *Chem. Phys. Lett.*, 2001, **337**, 341–348.

14 T. W. Keal and D. J. Tozer, *J. Chem. Phys.*, 2003, **119**, 3015–3024.

15 T. W. Keal and D. J. Tozer, *J. Chem. Phys.*, 2004, **121**, 5654.

16 S. J. Vosko, L. Wilk and M. Nusair, *Can. J. Phys.*, 1980, **58**, 1200.

17 C. Lee, W. Yang and R. G. Parr, *Phys. Rev. B*, 1988, **37**, 785–789.

18 A. D. Becke, *The Journal of Chemical Physics*, 1988, **88**, 1053–1062.

19 J. P. Perdew, K. Burke and M. Ernzerhof, *Phys. Rev. Lett.*, 1996, **77**, 3865–3868.

20 A. D. Becke, *The Journal of Chemical Physics*, 1997, **107**, 8554–8560.

21 A. D. Becke, *The Journal of Chemical Physics*, 1993, **98**, 1372–1377.

22 J. Tao, J. P. Perdew, V. N. Staroverov and G. E. Scuseria, *Phys. Rev. Lett.*, 2003, **91**, 146401.

23 T. Helgaker, M. Jaszuński and K. Ruud, *Chem. Rev.*, 1999, **99**, 293–352.

24 T. Helgaker, P. J. Wilson, R. D. Amos and N. C. Handy, *J. Chem. Phys.*, 2000, **113**, 2983–2989.

25 S. Kvaal, U. Ekström, A. M. Teale and T. Helgaker, *J. Chem. Phys.*, 2014, **140**, 18A518.

26 S. M. Colwell and N. C. Handy, *Chemical Physics Letters*, 1994, **217**, 271 – 278.

27 Q. Zhao, R. Morrison and R. Parr, *Phys. Rev. A*, 1994, **50**, 2138.

28 Q. Wu and W. T. Yang, *J. Chem. Phys.*, 2003, **118**, 2498–2509.

29 A. M. Teale, S. Coriani and T. Helgaker, *The Journal of Chemical Physics*, 2010, **132**, 164115.

30 CFOUR, *a quantum chemical program package written by J.F. Stanton, J. Gauss, M.E. Harding, P.G. Szalay with contributions from A.A. Auer, R.J. Bartlett, U. Benedikt, C. Berger, D.E. Bernholdt, Y.J. Bomble, L. Cheng, O. Christiansen, M. Heckert, O. Heun, C. Huber, T.-C. Jagau, D. Jonsson, J. Jusélius, K. Klein, W.J. Lauderdale, D.A. Matthews, T. Metzroth, L.A. Mück, D.P. O'Neill, D.R. Price, E. Prochnow, C. Puzzarini, K. Ruud, F. Schiffmann, W. Schwalbach, C. Simmons, S. Stopkowicz, A. Tajti, J. Vázquez, F. Wang, J.D. Watts and the integral packages MOLECULE (J. Almlöf and P.R. Taylor), PROPS (P.R. Taylor), ABACUS (T. Helgaker, H.J. Aa. Jensen, P. Jørgensen, and J. Olsen), and ECP routines by A. V. Mitin and C. van Wüllen. For the current version, see http://www.cfour.de.*

31 *Dalton, a molecular electronic structure program, Release Dalton2015.0 (2015), see http://daltonprogram.org.*

32 K. Aidas, C. Angeli, K. L. Bak, V. Bakken, R. Bast, L. Boman, O. Christiansen, R. Cimiraglia, S. Coriani, P. Dahle, E. K. Dalskov, U. Ekström, T. Enevoldsen, J. J. Eriksen, P. Ettenhuber, B. Fernández, L. Ferrighi, H. Fliegl, L. Frediani, K. Hald, A. Halkier, C. Hättig, H. Heiberg, T. Helgaker, A. C. Hennum, H. Hettema, E. Hjertenæs, S. Høst, I.-M. Høyvik, M. F. Iozzi, B. Jansík, H. J. Aa. Jensen, D. Jonsson, P. Jørgensen, J. Kauczor, S. Kirpekar, T. Kjærgaard, W. Klopper, S. Knecht, R. Kobayashi, H. Koch, J. Kongsted, A. Krapp, K. Kristensen, A. Ligabue, O. B. Lutnæs, J. I. Melo, K. V. Mikkelsen, R. H. Myhre, C. Neiss, C. B. Nielsen, P. Norman, J. Olsen, J. M. H. Olsen, A. Osted, M. J. Packer, F. Pawlowski, T. B. Pedersen, P. F. Provasi, S. Reine, Z. Rinkevicius, T. A. Ruden, K. Ruud, V. V. Rybkin, P. Sałek, C. C. M. Samson, A. S. de Merás, T. Saue, S. P. A. Sauer, B. Schimmelpfennig, K. Sneskov, A. H. Steindal, K. O. Sylvester-Hvid, P. R. Taylor, A. M. Teale, E. I. Tellgren, D. P. Tew, A. J. Thorvaldsen, L. Thøgersen, O. Vahtras, M. A. Watson, D. J. D. Wilson, M. Ziolkowski and H. Ågren, *WIREs Comput. Mol. Sci.*, 2015, **4**, 269–284.

33 *LONDON, an ab-initio program package for calculations in finite magnetic fields, founded by E. I. Tellgren, A. Soncini and T. Helgaker. Programming by E. I. Tellgren (main programmer), K. K. Lange, A. M. Teale, U. E. Ekström, S. Stopkowicz and J. H. Austad.*

34 E. I. Tellgren, A. Soncini and T. Helgaker, *J. Chem. Phys.*, 2008, **129**, 154114.

35 S. N. Maximoff and G. E. Scuseria, *Chem. Phys. Lett.*, 2004, **390**, 408–412.

36 E. Sagvolden, U. Ekström and E. Tellgren, *Mol. Phys.*, 2013, **111**, 1295–1302.

37 J. F. Dobson, *J. Chem. Phys.*, 1993, **98**, 8870.

38 A. D. Becke, *J. Chem. Phys.*, 2002, **117**, 6935.

39 J. Tao, *Phys. Rev. B.*, 2005, **71**, 205107.

40 J. E. Bates and F. Furche, *J. Chem. Phys.*, 2012, **137**, 164105.

41 J. W. Furness, J. Verbeke, E. I. Tellgren, S. Stopkowicz, U. Ekström, T. Helgaker and A. M. Teale, *In preparation (arXiv:1505.07989 [physics.chem-ph])*, 2015.